

## Stacking faults in colloidal crystals grown by sedimentation

Jacob P. Hoogenboom,<sup>a)</sup> Didi Derks, Peter Vergeer,<sup>b)</sup> and Alfons van Blaaderen<sup>a)</sup>  
*FOM Institute for Atomic and Molecular Physics, Kruislaan 407, 1098 SJ, Amsterdam, The Netherlands*  
*and Soft Condensed Matter, Debye Institute, Utrecht University, Princetonplein 5, 3584 CC Utrecht, The Netherlands*

(Received 17 July 2002; accepted 26 September 2002)

A real-space study is presented on the occurrence of stacking faults in crystals of silica colloids with diameters of about 1 and 1.4  $\mu\text{m}$  formed through sedimentation. The softness of the interaction potential is varied from slightly repulsive to hard-sphere like, both intrinsically by variation of the diameter, as well as through the addition of salt, which screens the surface charges. Our results indicate that the equilibrium crystal structure for these colloids is an fcc-crystal, with the number of stacking faults determined by the interplay between sedimentation and crystallization kinetics, irrespective of the softness of the interaction potential. For spheres with a certain diameter the number of stacking faults decreases with decreasing initial volume fractions. These results provide a way to grow fcc-crystals of hard-sphere particles by slow sedimentation. The relative number of stacking faults in the first few layers above the bottom wall can be as much as a factor of 10 higher than deeper into the crystal. This effect is due to the crystallization kinetics on a plain wall in a gravitational field. A patterned bottom wall that favors a specific hexagonal orientation was found to drastically reduce the number of stacking faults in the crystal. © 2002 American Institute of Physics. [DOI: 10.1063/1.1522397]

### I. INTRODUCTION

The ability of colloidal particles to self-assemble into a variety of crystalline phases lies at the heart of many materials-science studies, especially in the fields of photonics,<sup>1–3</sup> catalysis,<sup>4</sup> sensors<sup>1</sup> and lithography.<sup>5</sup> In these applications the colloids can either serve directly as the functional building block<sup>1,2,5</sup> or they form a template for making so-called inverse-opal structures.<sup>3,4,6</sup> For most applications, especially in the field of photonic materials, knowledge of and control over the formation of defects is crucial. First, the uncontrolled formation of defects destroys most optical characteristics, for instance by broadening and doubling of Bragg peaks.<sup>7,8</sup> Second, the controlled incorporation of defects may again be useful for instance by creating specific, localized defects modes. Considerable research has been devoted to the creation of such materials, but much less work focuses on the occurrence of defects. Recently, several papers discussed the influence of stacking faults, the most common type of defect in hard-sphere-like colloidal crystals, on the photonic properties of colloidal inverse-opal materials.<sup>7,8</sup> However, a detailed knowledge of the parameters that influence the formation of defects like stacking faults in colloidal materials is still lacking.

More research has been devoted to the occurrence of stacking faults in the hard-sphere model system from a theoretical point of view. This is mostly due to the almost degenerate nature of different close-packed hard-sphere stacking sequences and the related question as to what is the

stable crystal structure. The free energy differences between face-centered cubic (fcc), hexagonal close packed (hcp), and crystals exhibiting an arbitrary number of randomly distributed stacking faults, solely arise from entropic interactions. These free-energy differences have only recently been calculated using computational methods and are only on the order of  $10^{-4}k_B T$  per sphere at the melting volume fraction, where  $k_B$  is Boltzmann's constant.<sup>9–11</sup> The fcc crystal is the most stable structure, but these differences are so small that stacking faults can easily occur. Furthermore, Pronk and Frenkel demonstrated that when a finite crystallite size is taken into account a completely randomly stacked sequence [denoted as random hexagonal close packed (rhcp)] is more stable for crystallites containing less than about 30 000 particles.<sup>10</sup> This is an important consideration for experimental situations where often a polycrystalline state results or where the start of crystallization is examined. The subsequent relaxation from rhcp to fcc is estimated to be slow, on a time scale of months to years for 200 nm-diameter particles, and is furthermore predicted to be dependent on the grain-size.<sup>10</sup> In recent computer simulations, the crystal nuclei in a super-saturated liquid were found to be of rhcp type.<sup>12</sup>

Several experimental papers confirm this scenario. Zhu and co-workers found in space, thus without the influence of gravity, a pure rhcp stacking.<sup>13</sup> Most papers dealing with crystals nucleated on earth under conditions of bulk crystallization also report a strong tendency towards a random stacking,<sup>14–17</sup> however, the actual number of stacking faults as compared to the fcc structure can differ considerably upon method of preparation and the relaxation time after crystal nucleation.<sup>17</sup>

Research on the structure of colloidal crystals has mostly been performed using light scattering<sup>14,17,18</sup> or other diffrac-

<sup>a)</sup>Authors to whom correspondence should be addressed. Electronic mail: hoogenboom@amolf.nl; Electronic mail: a.vanblaaderen@phys.uu.nl

<sup>b)</sup>Currently at the Chemistry of Condensed Matter group at the address of the second affiliation.

tion methods.<sup>19</sup> With these techniques a well-averaged structure factor is obtained from which for instance the stacking sequence can only be obtained by performing a *global* fitting procedure, despite the fact that the occurrence of faults may vary throughout the crystal.<sup>7,10</sup> The recent rise of quantitative three-dimensional (3D) microscopy methods in colloid science<sup>20,21</sup> has also led to papers in which the stacking sequence was probed directly in real-space.<sup>15,16,22</sup> Furthermore, Gu and co-workers used confocal microscopy to illustrate the quality of their dried crystals, but they did not present an analysis of defects or stacking faults in their crystals.<sup>23</sup> Clearly, the question of getting reasonable statistical accuracy in a real-space analysis is of importance compared to diffraction methods—see, e.g., the large error margins reported in Ref. 15—but it has the big advantage of determining the stacking sequence *in situ*. Furthermore, by making clever use of the information provided by specific crystal orientations, stacking-fault counting can be simplified considerably.<sup>16</sup> Complementary to the previously mentioned papers, we will in this paper show the usefulness of real-space measurements by also probing the *location* of stacking faults. This will be done for a system of silica colloids that crystallized during sedimentation. Colloidal crystallization by sedimentation is one of the most commonly used techniques for making colloidal crystals for applications.<sup>3,4,6</sup> As such, the results presented here will be a first step towards a better understanding of and control over defect formation in photonic crystals. Moreover, several papers have claimed proofs for fcc crystallization of sedimented, charge-stabilized silica colloids and related these observations to hard-sphere behavior.<sup>24</sup> Here, we will also address the role of the “softness” of the interactions between the particles on the stacking sequence of colloidal crystals.

Crystallization during sedimentation is a situation much different from the zero-gravity or nearly zero-gravity systems mentioned previously. In fact, many of the “deviations” reported in those papers—i.e., the occurrence of a higher stacking sequence than pure rhcp—have been ascribed to the presence of a gravitational field, e.g., through gravity-induced shear or hydrodynamic interactions during settling, be it that its magnitude was low.<sup>13,17</sup> The magnitude of the gravitational field is usually described by the Peclet number,  $Pe = \Delta\rho g R^4 (kT)^{-1}$ , which expresses the gravitational energy relative to the thermal energy. For small Peclet numbers, typically  $Pe = O(10^{-4})$  corresponding to colloids with a radius of about 100 nm, the variation of volume fraction in the region above the sediment, which is called the “fan,” is rather smooth. In this case, the growth of the sediment can be well described by conventional hard-sphere crystal growth from the supersaturated solution just above the sediment.<sup>25</sup> For larger spheres, for instance with a radius of about 500 nm, the Peclet number is two orders of magnitude higher. Thus, the one-dimensional (1D) gravitational force-field has a much larger influence on crystallization. The influence of a strong 1D force field on crystallization has been only recently addressed.<sup>26,27</sup>

Apart from the presence and influence of gravity on the crystallization of sedimenting colloids, the presence of a substrate wall on which crystallization occurs also influences the

behavior of the colloidal suspension prior to and during crystallization.<sup>27–29</sup> For crystallization at a patterned wall, the occurrence of the best quality crystal with respect to the amount of defects, is, due to the presence of gravity, determined by the prefreezing and/or wetting behavior of the colloidal liquid.<sup>30</sup>

The conditions for obtaining a crystalline sediment for colloids at high Peclet-numbers are not immediately straightforward. At initial volume fractions  $\varphi_0 \sim 10^{-1}$  commonly used for sedimentation experiments with smaller, low Peclet-number particles ( $Pe \sim 10^{-1}$ ), spheres with a radius higher than about 400 nm do not form a crystalline sediment anymore.<sup>25</sup> This gave rise to some remarks that it would not be possible to crystallize colloids in this size-range by sedimentation,<sup>31</sup> but clearly this should be a matter of the balance between the particle flux due to sedimentation and the maximum growth velocity of the crystal. This balance can be tuned by slowing down sedimentation with an electric field like the authors of Ref. 31 did, but can also be tuned by adjusting the intrinsic parameters of the sedimentation process, like the initial volume fraction. There are indications from electron microscopy data that the amount of fcc-stacking in crystals of sedimenting colloids can be rather high.<sup>24</sup> It remains however unclear whether this is due to a softer interaction potential compared to hard-spheres caused by repulsive interactions between surface charges that are not completely screened, or whether it is due to the crystal growth kinetics or to the presence of the gravitational force-field directed towards the hard bottom wall.

In this paper we will investigate the occurrence of stacking faults in colloidal silica crystals grown by sedimentation. We will show that there is a finite number of stacking faults, but that the overall stacking parameter has a large tendency towards fcc. Furthermore, for a given particle size and interaction potential, the number of stacking faults decreases with decreasing initial volume fraction. This study is carried out using real-space measurements that allow for a direct determination of stacking faults, as well as their location. In the first few layers of the crystal over the bottom wall, we find an increased probability for stacking faults to occur, which also decreases on further reduction of the initial volume fraction. In addition to recent results showing the possibility to epitaxially grow any desired stacking sequence by using a template that directly dictates the stacking sequence,<sup>30</sup> the occurrence of stacking faults is also shown to be influenced by a wall pattern that favors a specific hexagonal orientation of crystal planes.

The remainder of this paper is organized as follows. First we will present the details of our experiments and of the structural analysis of the colloidal crystals. Then we will take a closer look at the sedimentation process in a colloidal system, as related to crystallization in the sediment. The section containing the results and the discussion of these results is divided in four parts. First, the behavior of the overall stacking parameter in the two systems investigated in detail will be presented. Then several additional experiments that examine the influence of surface charge screening through the addition of varying amounts of salt will be presented. The location of stacking faults as a function of the distance to the

TABLE I. Stacking parameters for the four different systems investigated in this study.<sup>a</sup>

$R$ (nm)	$d_{\text{HS}}/d$	$\varphi_0$	$Pe$	$(\varphi_0 Pe)^{-1}$	$\langle \alpha \rangle$	$\langle \alpha \rangle_{L>4}$
499	1.322	0.004	0.13	$2.5 \cdot 10^3$	$0.90 \pm 0.13$	$0.95 \pm 0.05$
499	1.322	0.002	0.13	$5.0 \cdot 10^3$	$0.94 \pm 0.07$	$0.97 \pm 0.02$
692	1.027	0.005	0.50	$0.4 \cdot 10^3$	$0.78 \pm 0.11$	$0.81 \pm 0.08$
692 <sup>b</sup>	1.027	0.005	0.50	$0.4 \cdot 10^3$	$0.91 \pm 0.07$	$0.91 \pm 0.06$

<sup>a</sup> $R$  is the sphere radius,  $d_{\text{HS}}/d$  is a measure for the softness of the interaction potential and gives the effective hard-sphere diameter over particle diameter,  $\varphi_0$  the initial volume fraction,  $Pe$  stands for the Peclet number, and  $\langle \alpha \rangle$  and  $\langle \alpha \rangle_{L>4}$  are the overall stacking parameter and the stacking parameter averaged over layers five and higher (counted from the bottom wall), respectively.

<sup>b</sup>Particles sedimented on a patterned wall that favors a single hexagonal orientation.

bottom wall comprises the third part of this section, followed by results on the influence of a surface pattern at the bottom wall on the stacking parameter.

## II. EXPERIMENT

Silica colloids that contained a fluorescently labeled core and a nonfluorescent shell were prepared using methods reported in the literature.<sup>32</sup> Particles with an outer radius of 499 nm as measured by transmission electron microscopy (TEM) contained a 100 nm-radius core that was labeled with rhodamin isothiocyanate (RITC).<sup>33</sup> The polydispersity, defined as the relative width of the size distribution, of these particles was 0.033. Particles with an outer radius of 692 nm, measured with TEM, contained a 192 nm-radius core labeled with fluorescein isothiocyanate (FITC). The polydispersity of these particles was 0.015.

For both batches, the particles were dispersed in a refractive-index matching mixture of demineralized water and glycerol (Baker, z.A grade) in a volume ratio of 1:7.18. In some of the experiments with the 692 nm-radius particles, N,N-dimethylformamide (DMF, Merck) and a refractive index matching mixture of 3:7 (volume ratio) DMF and dimethylsulfoxide (DMSO, Merck) were used. In order to screen interactions lithiumchloride (Merck) salt was added. Below we will explicitly mention which results have been retrieved with DMF, DMF-DMSO, and mixtures with salt added. For all other experiments, the water-glycerol mixture without added salt was used.

For the 499 nm-radius colloids, the bottom of the sedimentation container consisted of a 22 mm-diameter Chance no. 1 coverslip, which had been immersed in chromosulfuric acid (Merck) for 20 minutes and rinsed with demineralized water and ethanol (Merck, absolute grade) before being coated with a layer of poly(methylmethacrylate) (PMMA) to prevent particle adhesion. PMMA (950k, 4 wt% in chlorobenzene, MicroChem Corp.) was spin-coated at 1000 rpm for 30 s and subsequently baked for 1 hour at 170°C. This results in a layer thickness of  $\sim 450$  nm. A bottomless flask with an internal diameter of 9.65 mm was glued to the PMMA-coated coverslip using Silicon Rubber Adhesive RTV 102 (General Electric). The sedimentation container was rinsed several times with the water-glycerol mixture before filling it with a low-volume fraction suspension of colloids. For the 692 nm-radius spheres the sedimentation

container was similar, except that parts of the PMMA bottom wall had been patterned with an hcp(1100)-template using electron-beam lithography.<sup>30</sup>

The 499 nm-radius particles were dispersed at two different volume fractions,  $\varphi_0 = 0.004$  and  $\varphi_0 = 0.002$ . The 692 nm-radius particles were sedimented from a  $\varphi_0 = 0.005$  suspension (see Table I). The Peclet-numbers,  $Pe = \Delta\rho g R^4 (kT)^{-1}$ , for these two sizes are, respectively, 0.13 for the 499 nm-radius colloids and 0.5 for the 692 nm-radius colloids. Note that the water-glycerol mixture that was used has a rather high viscosity ( $\sim 10^2$  mPa·s), so the time scale of settling is scaled up considerably, but this does not affect the interplay between crystallization and sedimentation as both the settling speed as well as Brownian diffusion, and thus the rate of crystallization, are inversely proportional to the viscosity.

In order to quantify the softness of the interaction potential, the effective hard-sphere diameter,  $d_{\text{HS}}$ , in the bottom part of the sediment was determined. This value was determined from the interparticle spacing as calculated from confocal microscopy data (see below). The confocal diameter was then multiplied by the volume fraction, relative to 0.74, that a hard-sphere system with the same initial volume fraction, Peclet number, and overall sample volume would have. In calculation of the reference hard-sphere volume fraction, we use the fact that the osmotic pressure at the bottom of the sample balances the gravitational pressure. This value for  $d_{\text{HS}}$  was compared to the diameter,  $d$ , of the particles. The ratio  $d_{\text{HS}}/d$  for each of our samples is also indicated in Table I. The dependence of hard-sphere volume fraction on the distance from the bottom wall was determined as well, as described in Ref. 34. At the maximum depth in the crystal that was used to determine the stacking sequence, the volume fraction was always almost similar to the volume fraction at the bottom, i.e., higher than 0.70.

Samples were analyzed using fluorescence confocal microscopy (Leica TCS SP2) two months after homogenization of the dispersion. The samples were scanned in  $xy$ - and  $xz$ -mode, i.e., parallel and perpendicular to the bottom wall of the container respectively (the  $z$  direction is along the optical axis, while the  $x$  and  $y$  directions are the lateral coordinates parallel to the bottom wall). Crystallization of hard-sphere like colloids at a wall yields crystals that are oriented with their densest plane, an hexagonally packed layer, parallel to the wall. The stacking sequence of close-packed layers on top of each other can be easily probed by evaluation of par-

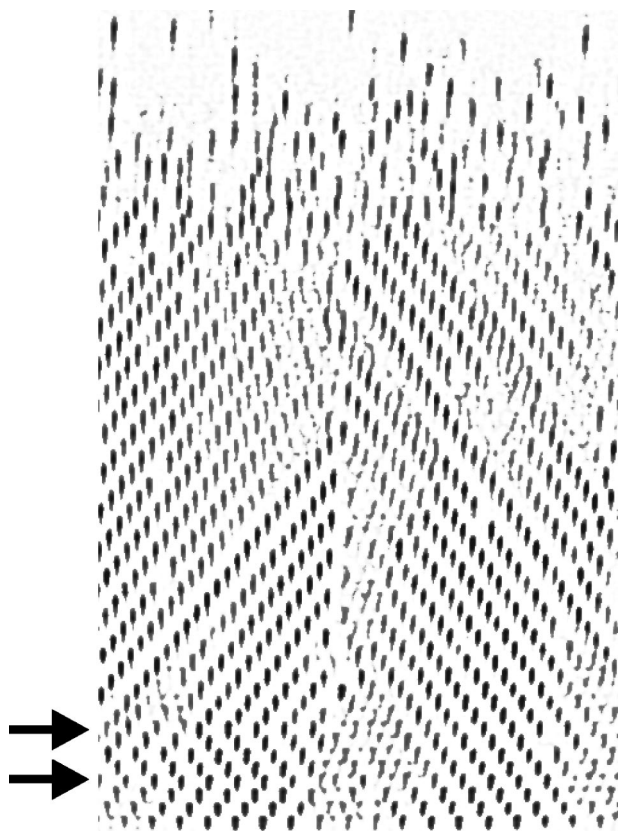


FIG. 1. Confocal image of a (110)-plane in two adjacent grains in a sedimented crystal. The optical axis of the microscope runs in the vertical direction. The elongated shape of particle images results from the different form of the points spread function parallel and perpendicular to the optical axis. The arrows indicate two stacking faults in the left grain that are visible as a kink. At the top of the image the fluidlike tail of the colloidal sediment profile is visible. The change in focus for different particles results from a small tilt of the sample with respect to the optical axis.

ticles positions in the (110)-plane,<sup>16,21</sup> perpendicular to the bottom wall. In fact, by using a template for crystal growth that carries a pattern of holes with similar symmetry as the (110)-positions in a crystal with a specific stacking sequence, a crystal with this hard-sphere stacking sequence can be grown.<sup>30</sup> In the Leica TCS SP2-system the scan field can be rotated. In this way the  $xz$ -scan can be chosen to coincide with the (110)-plane (see Fig. 1), which allows for an easy and fast way to probe crystal stacking. The elongated appearance of particles in Fig. 1 results from the decreased resolution along the optical axis of the microscope. The use of core-shell particles makes it however possible to clearly distinguish separate particles. Note that the fact that two adjacent crystal grains are displaying their (110)-plane in the same projection is purely coincidental.

The stacking sequence of hexagonal layers is usually denoted with the letters *A*, *B*, and *C*. If the positions in a specific layer are denoted by *B* then there are two sets of possible positions for both the layer above and the layer below, which are the *A*- and *C*-positions. Given the positions of the layer below as *A*, the layer atop can either have the same lateral coordinates, resulting in an *ABA*- or hexagonal close packed (hcp)-type stacking, or it can occupy the third set of coordinates *C*, which results in an *ABC*- or face cen-

tered cubic (fcc)-stacking. To each layer *i* in the crystal a value  $\sigma_i = \{0,1\}$  can now be assigned depending on its environment. If the stacking is fcc-type  $\sigma_i = 1$  and if it is hcp-type  $\sigma_i = 0$ . For a crystal consisting of *N* layers, this results in *N*-2 different  $\sigma_i$  (for the bottom and top layer  $\sigma_i$  is not defined), and the overall stacking parameter  $\alpha$  of the crystal can be calculated by averaging  $\sigma_i$ . In the (110)-plane an *ABA*-stacking is visible as a kink (indicated by the arrows in Fig. 1), so that determination of the stacking sequence comes down to counting the number of layers in the crystal as well as the number of kinks,  $\kappa$ . The stacking parameter  $\alpha$  of a crystal grain is thus given by<sup>16</sup>

$$\alpha = \frac{1}{N-2} \sum_{i=2}^{N-1} \sigma_i = 1 - \frac{\kappa}{N-2}.$$

For the two-crystal grains displayed in Fig. 1, this gives  $\alpha = 1$  and  $\alpha = 0.95$  for the right and left crystal, respectively. The overall stacking parameter of a sample is calculated as the total average  $\langle \alpha \rangle$  over the (110)-images taken of one sample. This averaging was performed with the value of  $\alpha$  for each stack calculated over the same number of layers,  $N = 22$ .

### III. SEDIMENTATION AND CRYSTALLIZATION

A description of a sedimentation process usually divides the sedimenting liquid into four regimes: A clear liquid on top, a part where colloids are freely settling at the initial volume fraction  $\varphi_0$ , the so-called fan in which there is a gradient in particle concentration from the initial volume fraction to the volume fraction at which particles accumulate at the bottom, the sediment.<sup>35</sup> The sedimentation velocity in the free settling regime is given by  $U(\varphi_0) = U_0 \cdot K(\varphi_0)$ , where  $U_0$  is the sedimentation velocity at infinite dilution and  $K(\varphi)$  is a volume-fraction dependent correction factor that takes into account the hindered motion at higher volume fractions. A good approximation of  $K(\varphi)$  for hard-spheres is given by  $K(\varphi) = (1 - \varphi)^{6.6}$ .

In the sediment the volume fraction is about 0.60 or higher (either in a compressed crystalline sediment or in a glassy sediment) and its structure can, depending on the kinetics of sedimentation versus crystallization, be crystalline or amorphous. In the fan above the sediment, the sedimentation velocity is dependent on the local volume fraction  $\varphi$  as given by  $K(\varphi)$ . The volume fraction at the bottom of the fan is equal to or higher than the melting volume fraction. The flux of particles into the sediment is independent of the initial volume fraction and is just given by the melting volume fraction times the corresponding sedimentation velocity. The sediment will crystallize as long as this flux equals the flux of particles into the crystal. The criterion for obtaining a crystallized sediment is that the sedimentation velocity at the bottom of the fan should be smaller than the maximum crystal growth velocity. As under similar conditions the sedimentation velocity is proportional to  $R^2$ , while the crystal growth velocity goes as  $R^{-2}$ , there is a maximum sphere radius above which the sediment does not crystallize anymore. This scenario was confirmed by Davis and co-workers who found

that for initial volume fractions on the order of  $10^{-1}$ , colloids with a radius of  $0.430 \mu\text{m}$  formed an amorphous sediment.<sup>25</sup>

This scenario holds as long as the particle flux from the free settling regime into the fan is higher than the maximum possible flux  $\varphi \cdot U(\varphi)$  for some value of  $\varphi$  between  $\varphi_0$  and the volume fraction of the sediment. In other words, when on the flux-curve [ $\varphi \cdot U(\varphi)$  versus  $\varphi$ ] the line connecting the starting point on the flux-curve (i.e., corresponding to the initial volume fraction) and the volume fraction of the sediment crosses the flux-curve. For hard-spheres this holds for initial volume fractions larger than about 0.02.<sup>35</sup> For smaller initial volume fractions the process is limited by the particle flux at the initial volume fraction. As the volume fraction at which the colloids crystallize is constant, the process can be described by the maximum rate of crystallization ( $\sim kT/R^2$ ), the initial rate of sedimentation ( $\sim \Delta\rho g R^2$ ) and the initial volume fraction  $\varphi_0$ . A proper parameter for characterizing the system is then  $kT/(\varphi_0 \Delta\rho g R^4) = 1/(\varphi_0 \cdot Pe)$ , assuming  $K(\varphi_0) \approx 1$ . This value is given in Table I for the different systems we have investigated.

## IV. RESULTS

### A. Overall stacking parameters

In Table I values for the overall stacking parameter,  $\langle\alpha\rangle$ , for the three systems with different  $(\varphi_0 Pe)^{-1}$  are given. As can be seen the values of  $\langle\alpha\rangle$  are rather high,  $>0.80$  for all three samples, indicating a strong preference for an fcc-stacking. These high stacking parameters are in strong contrast with results for hard-spheres in zero-gravity or under conditions of effective microgravity, where an almost pure rhcp-stacking ( $\langle\alpha\rangle \rightarrow 0.5$ ) is found. Furthermore it can be seen that the amount of stacking faults decreases with increasing  $(\varphi_0 Pe)^{-1}$ , from about 0.20 at  $(\varphi_0 Pe)^{-1} = 400$  to 0.06 at  $(\varphi_0 Pe)^{-1} = 5000$ . This indicates that the presence of stacking faults is to a large amount influenced by the kinetics of the sedimentation process and that by further decreasing of the initial volume fraction, thus increasing the equilibration time for the growing crystal, the resulting structure will be fcc.

The reason for the high amount of fcc-stacking maybe threefold: First, the presence of surface charges might give deviations from hard-sphere behavior. Secondly, the growth mechanism or the kinetics of the growth process might lead to a preference for fcc-stacking. Thirdly, the presence of a one-dimensional force field, i.e., gravity, possibly in combination with the presence of the bottom wall could favor the fcc stacking. We will discuss these three possibilities one by one.

#### 1. Repulsive versus hard-sphere interactions

Our silica particles are charge-stabilized with a steep, but not ideal hard-sphere, repulsion. This may change the behavior from that of hard-spheres and might give a tendency towards fcc, as fcc has been found to be the stable structure for colloids with long-ranged repulsive interactions at high volume fractions.<sup>36</sup> The softness of the interaction could explain the lower value of  $\langle\alpha\rangle$  for the 692 nm-radius particles, as for these larger particles the range of repulsion as expressed in

$d_{\text{HS}}/d$  (see Table I), is shorter. For a system with a softness of interactions in between our values, Gasser *et al.* reported rhcp crystallization in a nearly density-matched system.<sup>22</sup> In their work, they examined the structure of nucleating crystals, which will clearly be in the size range for which Pronk and Frenkel predicted rhcp to be the stable structure.<sup>10</sup> However, also measurements performed by Verhaegh *et al.* indicate an appreciable amount of stacking faults, higher than the values reported here, for a system of charged colloids.<sup>15</sup> Furthermore, the differences in the distribution of neighboring particles between fcc and hcp are very small and occur only at interparticle distances larger than  $1.63 \cdot d_{\text{HS}}$ . Thus short-ranged and smoothly varying potentials may be expected to give only a minor energy difference between the two structures. In fact, recent free-energy calculations indicate that the free-energy differences between hcp and fcc remain almost constant when increasing the softness of the interparticle potential.<sup>37</sup> This would mean that the origin of fcc-crystallization of long-ranged repulsive particles would be due to another reason than the contribution to the free-energy of a soft potential. In order to take a closer look at the effects of charge on the crystallization of sedimented silica colloids, some additional measurements with the 692 nm-radius particles were carried out. These results will be presented below, where we will come back to this point.

#### 2. Growth mechanism and growth kinetics

A second reason for the high amount of fcc-stacking in our crystals compared to hard-spheres in microgravity, may be the growth mechanism of the crystal nuclei. For the Lennard-Jones system, where differences between hcp and fcc are also negligibly small<sup>38</sup> but an fcc crystal structure is usually observed in simulations, growth mechanisms were suggested to explain fcc crystallization, for instance through an initial crossed stacking-fault that uniquely promotes fcc-growth.<sup>39</sup> As mentioned previously, at the Peclet-numbers examined in this research, the growth mechanism of crystals may be different from bulk crystallization. However, crystallization by sedimentation for similar silica colloids was recently shown to proceed via the growth of hexagonally stacked layers, with crystallization in a new layer starting with the formation of nuclei on top of already crystallized (111)-grains.<sup>27</sup> As an fcc-promoting growth mechanism would have to occur through either a nondegenerate crystal plane, or via self-repeating defects or surface steps, the growth mechanism can well be ruled out as the reason for the preference for fcc-stacking observed here. In fact, the growth mechanism in our system, which proceeds through stacking of (111)-planes, would seem the perfect growth mechanism for generating a heavily faulted crystal structure.

For this growth mechanism, the kinetics of growth however still play an important role, as was shown in the results given above. In bulk homogeneous crystallization the crystal growth rate is determined by the supersaturation. In fact, Pusey *et al.* already noted that the stacking parameter increased at lower supersaturation and thus lower rates of crystal growth.<sup>14</sup> In our system, the rate of crystal growth is uniquely determined by the initial volume fraction before sedimentation. By slowing down the sedimentation flux,

each crystal layer has more time to equilibrate, thus reducing the amount of crystal layers that get trapped in a metastable state, i.e., a stacking-fault.

### 3. The gravitational field and the bottom wall

A third reason for the high amount of fcc-stacking observed could be the influence of the one-dimensional asymmetry in the system, in the presence of the gravitational force field and the bottom wall, on the equilibrium crystal structure. As the particles used in this study have Peclet-numbers that are considerably larger than in previous studies, this could explain the increased tendency towards fcc. The influence of a one-dimensional force field on the equilibrium structure of hard spheres has not yet been investigated. Mau and Huse recently determined the strength of the entropic interactions between next-nearest close packed planes and further and found these differences to be very small.<sup>11</sup> This situation could however be different in the presence of a force field directed perpendicular to these close packed planes. Similarly, the surface free energy between a hard-sphere crystal and a hard wall was recently calculated,<sup>40</sup> but the influence of a hard wall on the structure of a hard-sphere crystal has, to our knowledge, also not been addressed yet.

### B. A closer look at surface charge screening

For the 692 nm-radius particles, additional measurements were carried out using both DMF and a refractive-index matching mixture of DMF and DMSO as a solvent, at high initial volume fractions of  $\varphi_0=0.052$  and  $\varphi_0=0.026$ . To both these solvents, small amounts of salt were added (order 1 mM), which changes the amount of screening of particle surface charges and thus changes the interaction towards more hard-sphere-like. From these additional experiments three important observations were made:

- (1) At an initial volume fraction of  $\varphi_0=0.052$ , only the sample without any salt added crystallized. In a sample with 2 mM of salt added, after sedimentation only small crystallites appeared on the bottom which extended only a few layers in the sample. The rest of the sample had a glasslike, disordered appearance. At a volume fraction of  $\varphi_0=0.026$  ( $1/(\varphi_0 \cdot Pe) \approx 80$ , so one order of magnitude lower than in Table I) all samples, with added salt concentrations ranging from 1 to 30 mM showed crystallization. From the interparticle distance at the bottom of the sediment after complete sedimentation, we found values for  $d_{HS}/d$  of  $d_{HS}/d=1.029$  in the samples with salt, compared to  $d_{HS}/d=1.140$  for the sample without salt.
- (2) We did not find any changes in the stacking parameter outside the error margins for all of these samples. The global stacking parameter was  $\langle \alpha \rangle = 0.67 \pm 0.10$ . Note that this is again substantially lower than the value of 0.78 in Table I for an order of magnitude higher value of  $1/(\varphi_0 \cdot Pe)$ .
- (3) The samples with salt added were all polycrystalline with a typical grain size of about 40  $\mu\text{m}$  wide (similar to the water-glycerol-dispersed samples in Table I). The

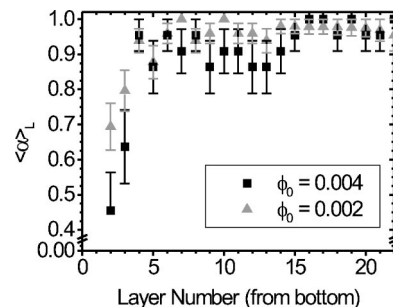


FIG. 2. Layer-averaged stacking parameter as a function of layer number from the bottom plane of the sample for a system of 1  $\mu\text{m}$  diameter silica colloids sedimented from volume fractions of 0.004 and 0.002.

samples without any salt added on the other hand showed crystallites with lateral sizes up to 500  $\mu\text{m}$ .

The lower stacking parameter in all of these samples confirms the trend in Table I. The result for  $\varphi_0=0.052$  shows that there is indeed an upper limit to the volume fraction needed to yield crystallization in the sediment at all. The increase in the range of the repulsion of the sample without salt lowers the sedimentation speed and affects the growth rate through the diffusion coefficient, which is enough to shift this limiting  $\varphi_0$  above  $\varphi_0=0.052$ . However, the influence on the kinetics of the process is not enough to increase the stacking parameter, at least not within the error margins. It does however influence the average domain size, which increases by an order of magnitude. Further research is needed, both theoretically as well as experimentally to study the effects of the softness of the interaction potential by slowly changing the interaction potential from hard-sphere-like to short-ranged and finally long-ranged repulsive. This should be performed first without the presence of gravity, but as mentioned before, the additional influence of the gravitational field and the presence of a hard bottom wall need to be investigated as well. Experimentally this could be done for small spheres at density-matching or at low Peclet number during sedimentation like in the work of Davis, Russel, and Glantschnig,<sup>25</sup> in a setup where it is possible to work with an ion-exchanged sample with the possibility to carefully control the amount of deionization.<sup>41</sup> The influence of the gravitational field can then be tested by comparing results on high Peclet-number samples.

### C. Location of stacking faults

For the samples given in Table I a layer-wise averaging of  $\alpha$  was carried out in order to probe a possible change in the number of stacking faults as a function of height in the sample. In Fig. 2  $\langle \alpha \rangle_L$  is shown for the two samples with 499 nm-radius particles for the first 22 layers in the crystal. Note that the data starts at layer 2 as the stacking parameter is not defined for the first layer in the sample. As can be seen  $\langle \alpha \rangle_L$  is for both samples remarkably lower in the second and third layer compared to higher in the sample. For layers four and higher the layer-wise averaged stacking parameter is constant within the error-margins.

The origin of the higher probability for the occurrence of stacking faults in the first three layers of a sedimented crystal may be kinetic. Previously, it became already evident that the kinetics of the sedimentation process influences the number of stacking faults in the crystals. Recently, we carried out a detailed analysis of the crystallization process at the wall during sedimentation, where it was found that the net osmotic pressure at which the first layer above the bottom wall crystallizes is higher than that for successive layers.<sup>27</sup> This effect leads to a decreased equilibration time for the first few layers in the sediment compared to layers higher in the sample. The relaxation time for each layer finally becomes a constant, fixed by the initial volume fraction and the sedimentation speed, and equal to the amount of time needed to add a number of particles to the sediment equal to the number of particles in one layer. The layer at which this happens is dependent on the difference in osmotic pressure at which the first and next layers crystallize. Our results indicated that this steady state was almost reached at crystallization of the fourth layer,<sup>27</sup> in correspondence with the results in Fig. 2. Furthermore, the fact that the number of stacking faults in layer two and three decreases when the initial volume fraction decreases, supports the notion that the effect has a kinetic origin and again stresses the importance of equilibration for the final crystal structure.

This effect is of importance for the use of sedimented colloidal crystals for photonic applications. For instance, thin crystals are sufficient to have a large bandgap,<sup>42</sup> but if conditions for colloidal crystal growth are then chosen such that there is an increased probability for stacking faults in the first few layers, this will have a strong effect on the photonic band structure. After the first four layers, the value for  $\langle\alpha\rangle_L$  seems to converge to a constant value for both two samples. The “converging” value of the stacking parameter for the bulk of the crystal was calculated by averaging over layers five and higher. These results are given in the last column of Table I. It should be noted that in view of the error margins on both values for  $\langle\alpha\rangle_{L>4}$ , we cannot exclude the possibility that the difference in stacking parameter for both volume fractions could be solely due to this bottom-layers effect. The difference between these samples and the 692 nm-radius samples would then be due to the difference in “hardness” of the interaction potential. However, the additional measurements for the 692 nm-radius particles also show an increase in stacking parameter upon decreasing initial volume fraction, while the bottom-layers effect can be expected to be smaller at these higher Peclet-numbers (also compare Figs. 2 and 3).

#### D. Influence of a bottom wall surface pattern

Finally, we want to illustrate how the interaction between the bottom wall and the crystallizing colloids influences the crystallization process and thus the stacking sequence as well. To this end, the stacking parameter was determined for the system of 692 nm-radius particles over a plain wall as well as over an hcp(1100)-patterned wall<sup>30</sup> that was mismatched in one direction. This pattern serves as a template for crystallization, lowering in the ideal case the surface free energy for a specific crystal orientation that then

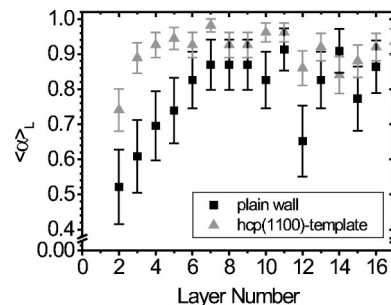


FIG. 3. Layer-averaged stacking parameter for a system of 1.4  $\mu\text{m}$  diameter silica colloids sedimented at a plain wall (black squares) and at a mismatched hcp(1100)-template, that gives rise to a fcc(111)-surface alignment.

nucleates. At this specific template crystallization occurs in hexagonally stacked layers oriented parallel to the bottom wall, just like on the unpatterned wall. However, the orientation of the crystal over the template was found to be uniform for larger crystallites (lateral sizes  $> 150 \mu\text{m}$ ) and only smaller crystallites (lateral sizes  $< 150 \mu\text{m}$ ) had a different orientation. At the plain wall crystallites had a typical lateral size of  $\sim 40 \mu\text{m}$ , without any apparent (i.e., by visual inspection) correlations in orientation. The measurements at the plain (untemplated) wall and the templated wall were performed in the same sample cell, so all further conditions are exactly similar.

In Table I the stacking parameter for the templated crystal is indicated as well. Furthermore, in Fig. 3 the layer-wise averaged stacking parameters are given for both templated and untemplated bottom wall. As can be seen, the overall stacking parameter on the templated wall is increased considerably with almost 20%. Furthermore, the increased probability for stacking faults to occur in the first few layers is also reduced with respect to the untemplated crystal. As there was such a clear distinction between smaller and larger crystallites, the stacking parameter over the templated wall was also analyzed as a function of grain-size. No stacking-faults were observed in the larger, template-oriented crystals, which were 6 crystallites out of a total of 67. For the smaller grains no correlation between crystallite size and the number of stacking faults was observed. More statistics is however needed to analyze the dependence of the stacking parameter on the crystal size, which is interesting in view of the stability of the rhcp structure for small crystals shown by Pronk and Frenkel.<sup>10</sup>

The comparison between crystals that crystallized at a plain wall and those that crystallized at a templated wall indicates that the interaction between the wall and the crystallizing suspension is of importance to the crystal quality as well. The effect of the bottom wall on the crystal structure plays a role through the surface free energy, so a change of  $\langle\alpha\rangle$  higher up in the crystal is not expected. In that respect the values for  $\langle\alpha\rangle_{L>4}$  in the last column of Table I can also be expected to be the “true” representation of the bulk stacking sequence. It would however still be interesting to test whether the favorable interaction of a template might be able to direct crystallization close to the wall to stacking-fault free fcc with the hexagonal fcc(111)-plane aligned parallel to the surface. This template might even be a simple hexagonal

patterned template as used by Heni and Löwen<sup>29</sup> in a recent simulation study of wetting and prefreezing in a hard-sphere system.

## V. CONCLUSIONS

A real-space analysis was performed on the crystal structure of sedimented silica colloids with Peclet-numbers on the order of  $10^{-1}$ . The softness of the interaction potential was furthermore varied from ratios between interparticle spacing and hard-sphere diameter of  $d_{\text{HS}}/d=1.027$  to  $d_{\text{HS}}/d=1.322$ . These crystals showed a remarkably high amount of fcc-stacking compared to bulk crystallization of hard-sphere particles. The tendency towards fcc may have two origins. It can be caused by the reduced crystal growth velocities compared to bulk homogeneous crystallization, which gives the growing crystal more time for equilibration, or it can be caused by the presence of the gravitational force field and the bottom wall of the sedimentation container which may favor fcc crystal structure. The amount of stacking faults is being reduced by changing the kinetics of sedimentation and crystallization through the initial volume fraction. The softness of the interactions is reflected in larger crystalline domain sizes, but does not seem to influence the global stacking parameter. Furthermore, the range of the interaction influences the kinetics of sedimentation and crystallization, which is reflected in the possibility to crystallize particles from a higher initial volume fraction than for more hard-sphere-like particles. Our results indicate that by slow sedimentation it is possible to grow fcc crystals of hard-sphere particles.

It was also shown that even under conditions where the stacking parameter towards the bulk of the crystal approaches values as high as 0.97, there is a remarkably higher probability for stacking faults to occur in the first four layers on top of the bottom wall. This decreased stacking parameter in the first few layers is also, at least partly, of kinetic origin and results from the different mechanism of crystallization, i.e., on a plain wall for the first layer and on top of an hexagonally packed lattice for layers two and further.

The importance of the free energy barrier for formation of the crystal layers at the bottom wall surface was shown by comparing the stacking sequence of silica particles sedimented on a plain wall with that on a template that favors a specific hexagonal orientation as reflected in larger domain sizes of oriented crystallites. Under similar conditions the overall stacking parameter is improved considerably towards fcc, from  $0.78 \pm 0.11$  to  $0.91 \pm 0.07$ . There are indications that, at this template, the smaller crystallites (with lateral size  $< 150 \mu\text{m}$ ) have a lower stacking parameter, but more statistics is needed to further investigate the size-dependence of the stacking sequence of colloidal crystals.

These results are important for people using sedimentation as a means to grow colloidal crystals for applications like photonic materials, as control over and decreasing of the amount of stacking faults is crucial for these applications. Our results also indicate the need for more extensive investigations, both theoretically as well as experimentally on heterogeneous crystal growth, both in the presence of gravity as well as without the gravitational field. This knowledge is

needed in order to understand and predict the phase behavior of colloids, but is furthermore crucial for the application and engineering of colloidal materials.

## ACKNOWLEDGMENTS

The authors would like to thank Stefan Auer and Sander Pronk (AMOLF) for a critical reading of this manuscript and for sharing their results prior to publication and Alexander Moroz (Utrecht University) for discussions. We also want to acknowledge a series of lectures given, amongst other subjects, on sedimentation by W. B. Russel (Princeton University) at the Debye Institute in Utrecht. This work is part of the research program of the ‘‘Stichting voor Fundamenteel Onderzoek der Materie (FOM),’’ which is financially supported by the ‘‘Nederlandse organisatie voor Wetenschappelijk Onderzoek (NWO).’’

- <sup>1</sup>S. A. Asher, J. Holtz, J. Weissman, and G. S. Pan, MRS Bull. **23**, 44 (1998).
- <sup>2</sup>A. van Blaaderen, K. P. Velikov, J. P. Hoogenboom, D. L. J. Vossen, A. Yethiraj, R. P. A. Dullens, T. van Dillen, and A. Polman, in *Photonic crystals and light localization in the 21st century*, edited by C. M. Soukoulis (Kluwer, Dordrecht, 2001), p. 239.
- <sup>3</sup>J. E. G. J. Wijnhoven and W. L. Vos, Science **281**, 802 (1998); A. A. Zakhidov, R. H. Baughman, Z. Iqbal, C. X. Cui, I. Khayrullin, S. O. Dantas, I. Marti, and V. G. Ralchenko, *ibid.* **282**, 897 (1998); A. Blanco, E. Chomski, S. Grabtchak *et al.* Nature (London) **405**, 437 (2000); Y. A. Vlasov, X. Z. Bo, J. C. Sturm, and D. J. Norris, *ibid.* **414**, 289 (2001).
- <sup>4</sup>B. T. Holland, C. F. Blanford, and A. Stein, Science **281**, 538 (1998).
- <sup>5</sup>H. W. Deckman and J. H. Dunsmuir, Appl. Phys. Lett. **41**, 377 (1982); F. Burmeister, W. Badowsky, T. Braun, S. Wieprich, J. Boneberg, and P. Leiderer, *ibid.* **145**, 461 (1999); C. L. Haynes and R. P. Van Duyne, J. Phys. Chem. B **105**, 5599 (2001).
- <sup>6</sup>A. Imhof and D. J. Pine, Nature (London) **389**, 948 (1997).
- <sup>7</sup>Y. A. Vlasov, V. N. Astratov, A. V. Baryshev, A. A. Kaplyanskii, O. Z. Karimov, and M. F. Limonov, Phys. Rev. E **61**, 5784 (2000).
- <sup>8</sup>V. Yannopoulos, N. Stefanou, and A. Modinos, Phys. Rev. Lett. **86**, 4811 (2001).
- <sup>9</sup>L. V. Woodcock, Nature (London) **385**, 141 (1997); P. G. Bolhuis, D. Frenkel, S. C. Mau, and D. A. Huse, *ibid.* **388**, 235 (1997); L. V. Woodcock, *ibid.* **388**, 236 (1997).
- <sup>10</sup>S. Pronk and D. Frenkel, J. Chem. Phys. **110**, 4589 (1999).
- <sup>11</sup>S. C. Mau and D. A. Huse, Phys. Rev. E **59**, 4396 (1999).
- <sup>12</sup>S. Auer and D. Frenkel, Nature (London) **409**, 1020 (2001).
- <sup>13</sup>J. X. Zhu, M. Li, R. Rogers, W. Meyer, R. H. Ottewill, W. B. Russel, and P. M. Chaikin, Nature (London) **387**, 883 (1997).
- <sup>14</sup>P. N. Pusey, W. van Meegen, P. Bartlett, B. J. Ackerson, J. G. Rarity, and S. M. Underwood, Phys. Rev. Lett. **63**, 2753 (1989).
- <sup>15</sup>N. A. M. Verhaegh, J. S. van Duijneveldt, A. van Blaaderen, and H. N. W. Lekkerkerker, J. Chem. Phys. **102**, 1416 (1995).
- <sup>16</sup>M. S. Elliot, B. T. F. Bristol, and W. C. K. Poon, Physica A **235**, 216 (1997).
- <sup>17</sup>W. K. Kegel and J. K. G. Dhont, J. Chem. Phys. **112**, 3431 (2000).
- <sup>18</sup>C. Dux and H. Versmold, Phys. Rev. Lett. **78**, 1811 (1997).
- <sup>19</sup>H. Versmold, Phys. Rev. Lett. **75**, 763 (1995); W. L. Vos, M. Megens, C. M. van Kats, and P. Bosecke, Langmuir **13**, 6004 (1997).
- <sup>20</sup>A. van Blaaderen, Progress in Colloid and Polymer Science **104**, 59 (1997); A. D. Dinsmore, E. R. Weeks, V. Prasad, A. C. Levitt, and D. A. Weitz, Appl. Opt. **40**, 4152 (2001).
- <sup>21</sup>M. S. Elliot and W. C. K. Poon, Adv. Colloid Interface Sci. **92**, 133 (2001).
- <sup>22</sup>U. Gasser, E. R. Weeks, A. Schofield, P. N. Pusey, and D. A. Weitz, Science **292**, 258 (2001).
- <sup>23</sup>Z. Z. Gu, A. Fujishima, and O. Sato, Chem. Mater. **14**, 760 (2002).
- <sup>24</sup>H. Míguez, F. Meseguer, C. Lopez, A. Mifsud, J. S. Moya, and L. Vazquez, Langmuir **13**, 6009 (1997); B. Y. Cheng, P. G. Ni, C. J. Jin,

- Z. L. Li, D. Z. Zhang, P. Dong, and X. C. Guo, *Optics Communications* **170**, 41 (1999).
- <sup>25</sup>K. E. Davis, W. B. Russel, and W. J. Glantschnig, *Science* **245**, 507 (1989).
- <sup>26</sup>T. Biben, R. Ohnesorge, and H. Löwen, *Europhys. Lett.* **28**, 665 (1994).
- <sup>27</sup>J. P. Hoogenboom, P. Vergeer, and A. van Blaaderen (unpublished).
- <sup>28</sup>D. H. Van Winkle and C. A. Murray, *J. Chem. Phys.* **89**, 3885 (1988); D. J. Courtemanche and F. Vanswol, *Phys. Rev. Lett.* **69**, 2078 (1992); M. Heni and H. Löwen, *J. Phys.: Condens. Matter* **13**, 4675 (2001).
- <sup>29</sup>M. Heni and H. Löwen, *Phys. Rev. Lett.* **85**, 3668 (2000).
- <sup>30</sup>J. P. Hoogenboom, A. K. van Langen-Suurling, J. Romijn, and A. van Blaaderen (unpublished).
- <sup>31</sup>M. Holgado, F. Garcia-Santamaria, A. Blanco *et al.*, *Langmuir* **15**, 4701 (1999).
- <sup>32</sup>A. van Blaaderen and A. Vrij, *Langmuir* **8**, 2921 (1992); H. Giesche, *J. Eur. Ceram. Soc.* **14**, 205 (1994).
- <sup>33</sup>N. A. M. Verhaegh and A. van Blaaderen, *Langmuir* **10**, 1427 (1994).
- <sup>34</sup>J. S. van Duijneveldt, J. K. G. Dhont, and H. N. W. Lekkerkerker, *J. Chem. Phys.* **99**, 6941 (1993).
- <sup>35</sup>W. B. Russel, D. A. Saville, and W. R. Schowalter, *Colloidal Dispersions* (Cambridge University Press, Cambridge, 1989).
- <sup>36</sup>E. B. Sirota, H. D. Ou-Yang, S. K. Sinha, P. M. Chaikin, J. D. Axe, and Y. Fujii, *Phys. Rev. Lett.* **62**, 1524 (1989); F. El Azhar, M. Baus, J. P. Ryc-kaert, and E. J. Meijer, *J. Chem. Phys.* **112**, 5121 (2000).
- <sup>37</sup>S. Auer and D. Frenkel, *J. Phys.: Condens. Matter* **14** (Peter Pusey's 60th birthday issue), 1 (2002).
- <sup>38</sup>A. N. Jackson, A. D. Bruce, and G. J. Ackland, *Phys. Rev. E* **65**, 036710 (2002).
- <sup>39</sup>B. W. Van de Waal, *Phys. Rev. Lett.* **67**, 3263 (1991).
- <sup>40</sup>M. Heni and H. Löwen, *Phys. Rev. E* **60**, 7057 (1999).
- <sup>41</sup>T. Palberg, W. Hartl, U. Wittig, H. Versmold, M. Wurth, and E. Simnacher, *J. Phys. Chem.* **96**, 8180 (1992).
- <sup>42</sup>K. Ohtaka and Y. Tanabe, *J. Phys. Soc. Jpn.* **65**, 2276 (1996).